

## Study of Transport Properties in Armchair Graphyne Nanoribbons: A Density Functional Approach

S. Golafrooz Shahri, M.R. Roknabadi,\* N. Shahtahmasebi, and M. Behdani

Department of Physics, Ferdowsi University of Mashhad, Mashhad, Iran

(Received September 1, 2015; revised manuscript received October 29, 2015)

**Abstract** In present paper, the non-equilibrium Green function (NEGF) method along with the density functional theory (DFT) are used to investigate the effect of width on transport and electronic properties of armchair graphyne ( $\gamma$ -graphyne) nanoribbons. The results show that all the studied nanoribbons are semiconductor and their band gaps decrease as the widths of nanoribbons increase, which will result in increasing current at a certain voltage. Also our results show the promising application of armchair graphyne nanoribbons in nano-electrical devices.

**PACS numbers:** 73.63.-b

**Key words:** transport properties, density functional theory, graphyne nanoribbons, non-equilibrium green function

### 1 Introduction

Carbon, the main composing element of earth, is capable of forming numerous allotropes due to its three distinct hybridized states, namely  $sp$ ,  $sp^2$  and  $sp^3$ .<sup>[1–2]</sup> Graphyne (Gy), as a new form of carbon non-natural allotrope, has been the subject of increasing studies because of its special structural, electrical, optical and mechanical properties. Gys, which were predicted by Baughman in 1987,<sup>[3]</sup> have the same symmetry as graphene with hexagonal carbon rings ( $sp^2$  hybridized C atom) and acetylenic linkage ( $sp$  hybridized C atom).<sup>[4]</sup> The presence of  $sp$  carbon atoms allows the formation of multiple lattice types of graphyne sheets with different symmetries called  $\alpha$ ,  $\beta$ ,  $\gamma$  and 6-6-12 graphyne.<sup>[5]</sup>

Recent theoretical researches indicated that Gys, due to acetylenic linkages, show versatile physical properties including have smaller carrier effective mass, higher carrier mobility and enhanced chemical properties; when compared with graphene.<sup>[6–10]</sup> The structural and electronic properties of graphyne nanoribbons (GyNRs), which would be formed by cutting Gy sheets, are strongly dependent on the edge chirality (armchair, zigzag) and their widths.

The theoretical studies on graphyne nanoribbons indicated that all armchair-edged  $\alpha$ -GyNRs ( $\alpha$ -AGyNRs) are nonmagnetic semiconductors, while the zigzag-edged  $\alpha$ -GyNRs ( $\alpha$ -ZGyNRs) are predicted to be antiferromagnetic (AFM) semiconductors,<sup>[1,11–12]</sup> with their band gaps depending on the width of ribbons.

The band gap of zigzag  $\gamma$ -GyNRs ( $\gamma$ -ZGyNRs) demonstrates a unique “step effect” by increasing its width.<sup>[13]</sup> These special properties of graphynes make them a promising candidate for optoelectronic devices, sensing applications and energy storage.<sup>[5,14–17]</sup>

In this paper, the electrical and transport properties of

armchair graphyne ( $\gamma$ -graphyne) nanoribbons were investigated using the first-principle calculations based on the density functional theory (DFT). To calculate the current-voltage (I-V) characteristics of the armchair  $\gamma$ -GyNRs, non-equilibrium Green functions theory coupled with the density functional theory [NEGF-DFT] were applied.

### 2 Method

In this study, the electrical and transport properties of armchair GyNRs are investigated by using density functional theory (DFT) as implemented in the OpenMx package,<sup>[18]</sup> where the generalized gradient approximation (GGA) and Perdew–Burke–Erzerhof (PBE)<sup>[19]</sup> were applied for exchange-correlation energy at room temperature (300 k).

In order to describe the interaction between the valance and core electrons, norm-conserved pseudopotential of Troullier–Martins and linear combinations of atomic orbital are used as the basis set. Also, a plane-wave basis set with a cut-off energy of 150 Ry is selected and k-point meshes are sampled using  $1 \times 1 \times 5$  k grid to describe Brillouin zone. Also,  $2s^2 2p^2$  electron configuration is taken to describe valance electrons of carbon atom. Lattice constant and all atomic coordinates are relaxed until the force on each atom dropped below  $0.02 \text{ eV}/\text{\AA}$ . A vacuum of about  $15 \text{ \AA}$  is set between the graphyne sheets to prevent their possible interactions with neighboring layers. It should be noted that there are two kinds of edge terminations: hexagon rings and acetylene linkages. In this study, the hexagon rings terminations whose dangling bonds are saturated by hydrogen are investigated.

To study the transport through nanoribbons, we consider a system with three parts: left lead ( $L$ ), central region ( $C$ ) and right lead ( $R$ ) (see Fig. 1). Moreover it is assumed that the left (right) lead is only coupled with the central region not the right (left) lead.

\*Corresponding author, E-mail: roknebad@um.ac.ir

The transport properties are obtained using the non-equilibrium Green functions [NEGF], where the Hamiltonian matrix is generated by DFT. The transmission function is calculated by the following formula,<sup>[22]</sup>

$$T(E) = \text{Tr} [\Gamma_L(E)G(E)\Gamma_R(E)G^\dagger(E)], \quad (1)$$

where  $G(E)$  is the Green's function calculated from the Hamiltonian and self-energies of the central region and  $\Gamma_\alpha(E)$  is the minus twice of imaginary part of self-energies of the left and right electrodes ( $\alpha = L, R$ ). The current is calculated by the Landauer–Buttiker formula:

$$I = \left(\frac{G_0}{e}\right) \int_{\mu_L}^{\mu_R} [f(E, \mu_L) - f(E, \mu_R)] T(E) dE, \quad (2)$$

where  $\mu_L$  and  $\mu_R$  are the chemical potentials of the left and right leads respectively,  $G_0 (= 2e^2/h)$  is the quantum of conductance and  $f(E)$  represents the Fermi–Dirac distributions of two leads with electrochemical potentials of  $\mu_L$  and  $\mu_R$ .<sup>[23]</sup> By applying voltage, the chemical potential of left/right electrode increases/decreases and transmission peaks that are related to electronic states contribute in current through nanoribbon.

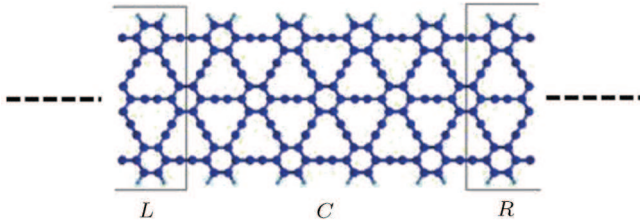


**Fig. 1** Schematic representation of the system for transport calculations.

### 3 Results

Before calculations of transport properties, the atomic coordinates are relaxed. The optimized structure indicates that the length of triple bond is 1.25 Å and the lengths of two single bonds are 1.42 Å and 1.44 Å (Fig. 2)

respectively, which is in good agreement with previous reports.<sup>[20–21]</sup>

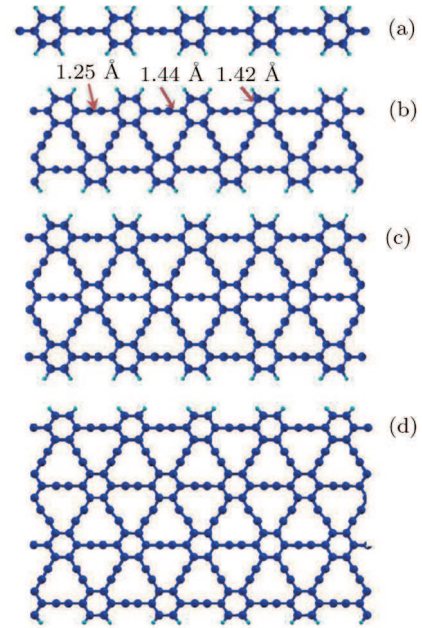


**Fig. 2** Schematic illustration of the (a)  $n = 1$ , (b)  $n = 2$ , (c)  $n = 3$ , and (d)  $n = 4$  armchair graphyne nanoribbons before relaxation.

At first, we studied the band structure [BS] and density of state [DOS] of armchair  $n$ -graphyne nanoribbons ( $n$ -AGyNR) where  $n$  indicates the number of hexagonal rings in the width of ribbons, as shown in Fig. 3. The results show that all ribbons are semiconductor, with an energy band gap in the range of about 0.8 eV to 1.6 eV, which calculated energy gaps are presented in Table 1. We found that the band gaps decrease as the width of ribbons grows in narrow ribbons, like graphene, which is in good agreement with other reports in Ref. [13].

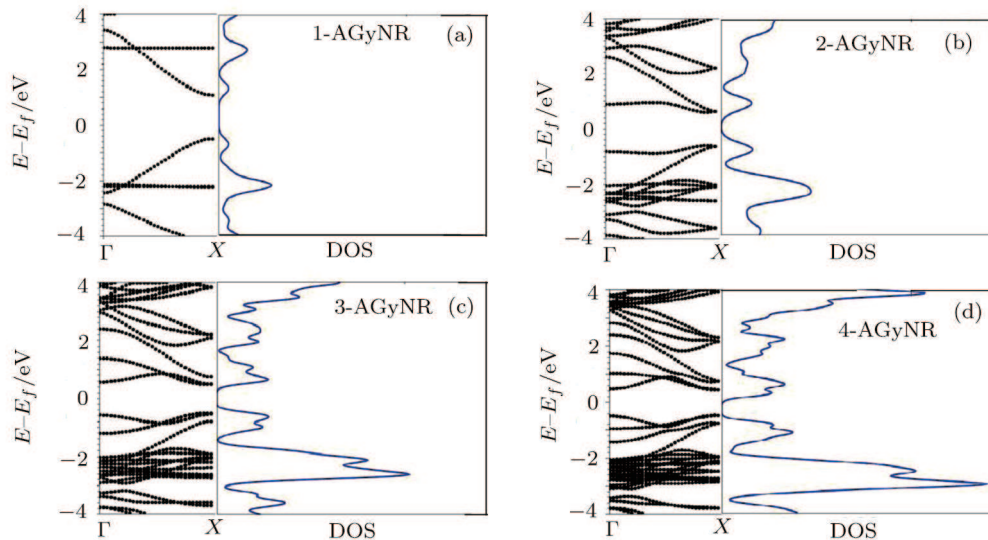


**Fig. 3** Band structure [BS] and density of state [DOS] of the (a)  $n = 1$ , (b)  $n = 2$ , (c)  $n = 3$ , and (d)  $n = 4$  armchair graphyne nanoribbons.

**Table 1** The calculated energy gap of all considered configurations as a function of ribbon width.

Width	$n = 1$	$n = 2$	$n = 3$	$n = 4$
$E_g/eV$	1.6	1.3	1.0	0.8

In addition, the band gaps are located near to the  $X$  point in the first Brillouin zone. Also in the band structure of 1-AGyNR around the Fermi level, one can see two bands with negligible band width which are related to quantum confinement effect and localized state on the edges of nanoribbons. The quantum confinement effect is observed when the size of the structure is too small to be comparable to the wavelength of the electron. So as the

size of a particle decreases till to nano scale the decrease in confining dimension makes the energy levels discrete and this increases or widens up the band gap and ultimately the band gap energy also increases. As can be seen in the next ribbons band structure, these effects are reduced by increasing the ribbons width.

Figure 3 shows the DOS per atom for  $n = 1$ ,  $n = 2$ ,  $n = 3$ , and  $n = 4$  of graphyne nanoribbons. The positions of DOS curves are in agreement with the electronic structures of ribbons. In Dos curves, as well, it can be observed sharp peaks around the Fermi level that they are correspond to localized state in band structure that mentioned before.

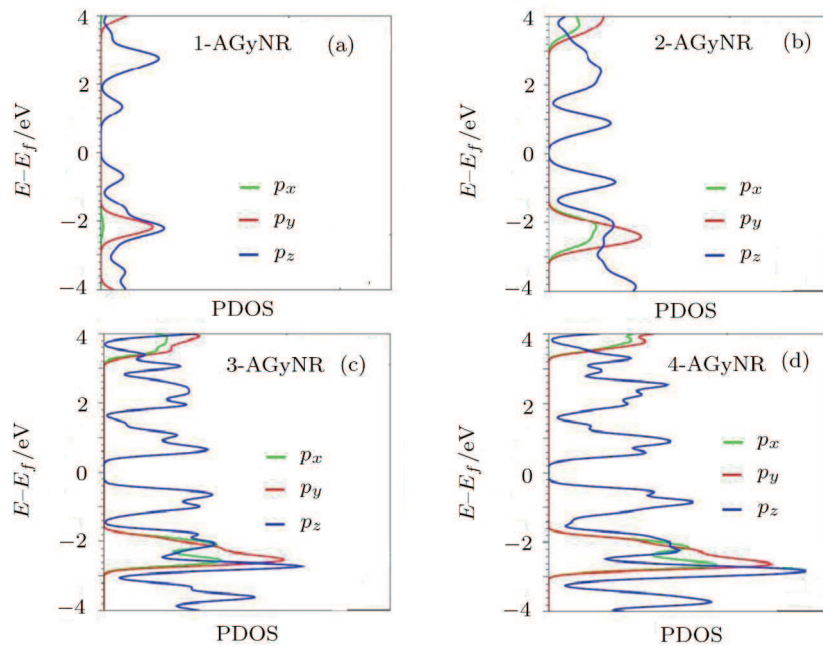


**Fig. 4** The PDOS spectrums of  $C$  atoms in the (a)  $n = 1$ , (b)  $n = 2$ , (c)  $n = 3$ , and (d)  $n = 4$  armchair graphyne nanoribbons.

To understand the bonding type, the projected density of states [PDOS] on the atomic orbitals ( $2s$ ,  $2p_x$ ,  $2p_y$ , and  $2p_z$ ) are obtained, as shown in Fig. 4. PDOS graphs show that the electronic states near Fermi energy are mainly of  $\pi$  type. This phenomenon is often observed in other graphyne nanoribbons, as well.<sup>[11–13]</sup>

The electronic states around Fermi level are  $\pi$  states that come from the hybridization between  $2p_z$  atomic orbitals. The contribution of other orbitals around the Fermi level is negligible. The unique transport properties of graphyne can be attributed to the electronic transport through  $\pi$  orbital, while the strong mechanical properties are derived from  $\sigma$  bonds. According to our results, a single orbital tight-binding model best suits the graphyne nanoribbons.

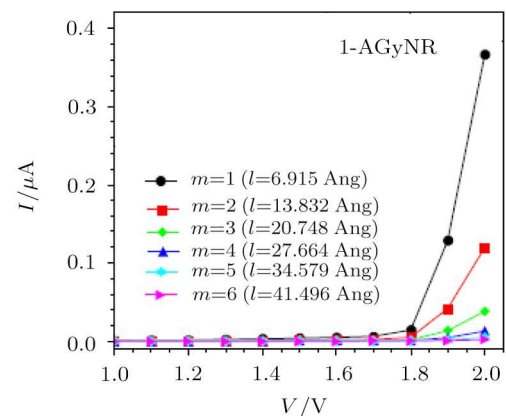


**Fig. 5** I-V curves for six different lengths of 1-AGyNR, that  $m$  indicates the number of hexagonal rings in the length of nanoribbon.

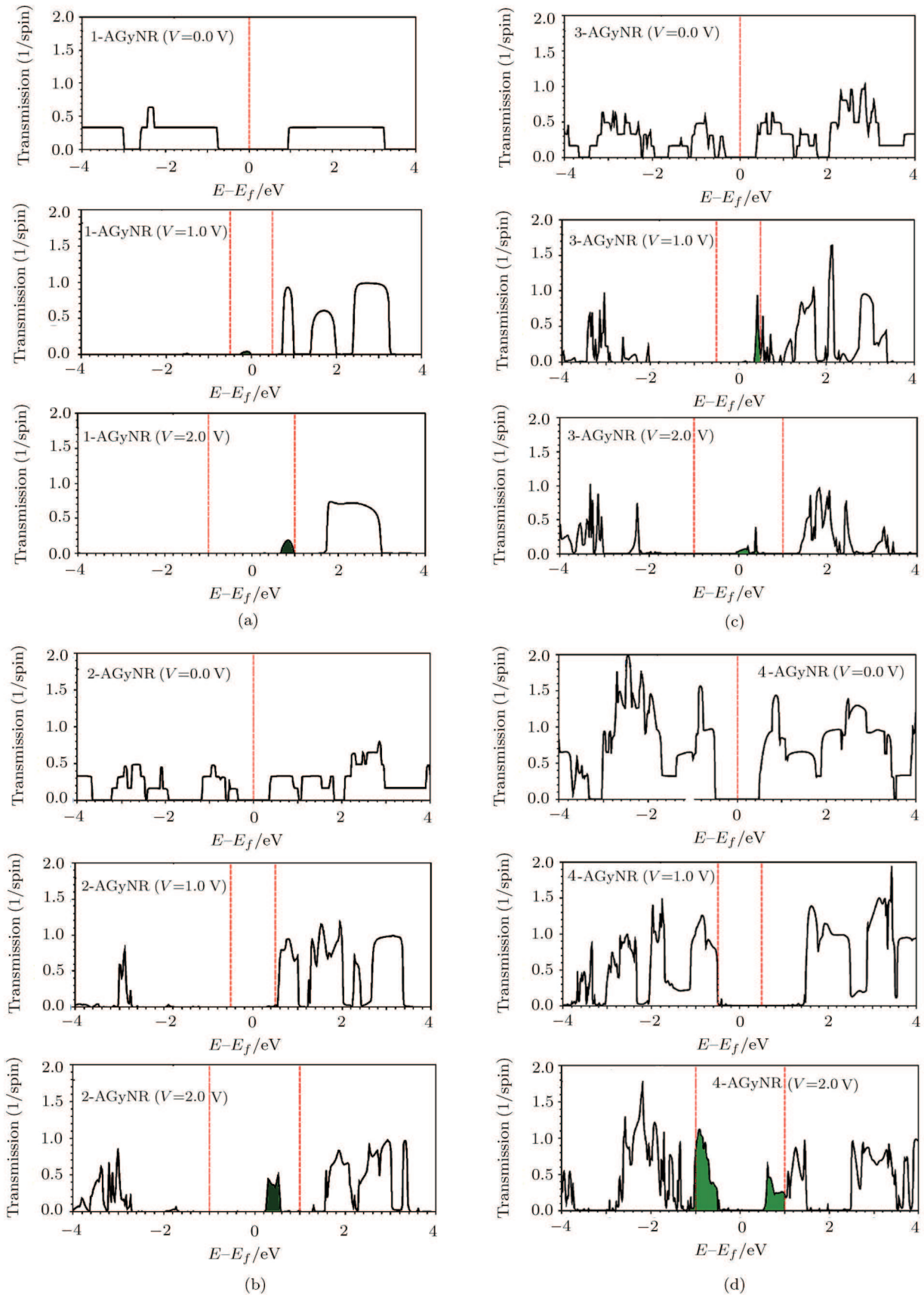


**Fig. 6** The total transmission spectrums of (a)  $n = 1$ , (b)  $n = 2$ , (c)  $n = 3$ , and (d)  $n = 4$  armchair graphene nanoribbons.

Before discussing about current changes as a function of applied bias voltage, it is worth to mention that the length of the ribbons at the scattering region strongly affects the transport properties of sample in non-equilibrium Green function method. For a short discussion on this topic, we calculate and plot the I-V curves for six different lengths of 1-AGyNR in Fig. 5. As expected, current decreases by increasing the length of ribbon. In the following calculations we use length of 20.748 Å for all considered nanoribbons.

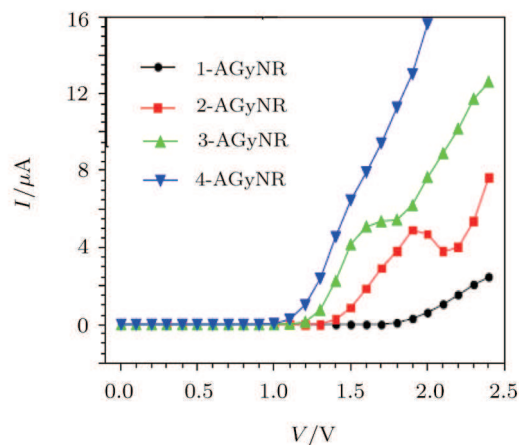


Fig. 7 I-V curves for armchair graphyne nanoribbons.

The transmission curves of  $n$ -AGyNR as a function of energy are plotted for different bias voltages (Fig. 6). The transmission peaks are corresponded to the eigenvalues of the nanoribbons. The analysis of each figure indicates that by increasing the bias voltage, new states are introduced to the nanoribbon, facilitating the transport through it. The solid red lines correspond to the energy window for each bias voltage. In the positive bias, the electronic states are localized resulting in sharper transmission peaks around certain energies, which are in fact the eigenvalues of the system. Also at these voltages, the HOMO/LUMO states shift transmission peaks toward/away from the Fermi energy.<sup>[24]</sup> The electronic

states localized by the external electric field, result in decrease of transmission.

In Fig. 7, I-V curves of  $n$ -AGyNR for a bias between 0.0 V and 2.5 V are presented. As it can be seen, the threshold voltages of  $n$ -AGyNR for  $n = 1$ ,  $n = 2$ ,  $n = 3$ , and  $n = 4$  are about 1.8 V, 1.4 V, 1.2 V, and 1.0 V, respectively. The current rises sharply when the bias voltage ( $V_b$ ) exceeds the threshold voltage. In the case of 2-AGyNR, the competition between the opening of energy window and localization, due to the external electric field, produces a negative slope in the current-voltage curve between 1.8 V and 2.0 V which is commonly known as the negative differential resistance (NDR).<sup>[25–26]</sup> By increasing the ribbon width, new conduction channel will be opened, resulting in increase of the current. I-V curves also verify the semiconducting characteristics of armchair graphyne.

#### 4 Conclusions

In this paper, the electronic transport properties of armchair  $\gamma$ -graphyne nanoribbons are studied. The results show that all armchair  $\gamma$ -graphyne nanoribbons have semi-conductive characteristics along the armchair direction. The transport properties of this family are similar to each other, in which by increase of nanoribbon width the band gap reduces while the current increases. In addition, the band gap positions were located near to the  $X$  point of the reciprocal space.

Furthermore, a threshold voltage is observed for each ribbon, which decreases by increasing the width of ribbon. However, it should be mentioned that the current increases when the bias voltage exceeds the threshold voltage.

The PDOS spectrum demonstrated that the unique transport properties of the ribbons could be attributed to the electronic transport through  $\pi$  orbitals.

The novel properties of graphyne nanoribbons, distinctive from those of graphene, make them a promising candidate for numerous applications in nanoelectronic devices.

## References

- [1] A. Hirsch, Nature (London) **9** (2010) 868.
- [2] W. Wu, W. Guo, and X.C. Zeng, Nanoscale **5** (2013) 9264.
- [3] M.Y. Han, B. Ozyilmaz, Y.B. Zhang, *et al.*, Phys. Rev. Lett. **98** (2007) 206805.
- [4] W.L. Ma and S.S. Li, Appl. Phys. Lett. **100** (2012) 163109.
- [5] A.L. Ivanovskii, Prog. Solid State Chem. **41** (2013) 1.
- [6] Y. Zhou, J. Zeng, and K.Q. Chen, Carbon **76** (2014) 175.
- [7] H.W. Kroto, J.R. Heath, S.C. O'Brien, R.F. Curl, and R.E. Smalley, Nature (London) **3** (1985) 318.
- [8] S. Iijima, Nature (London) **8** (1991) 354.
- [9] S. Tanuma, A.V. Palmichenko, and N. Satoh, Synthetic Met **4** (1995) 1841.
- [10] D. Wei, L. Xie, K.K. Lee, Z. Hu, S. Tan, and W. Chen, Nat. Commun. **4** (2013) 1374.
- [11] Y.W. Son, M.L. Cohen, and S.G. Louie, Phys. Rev. Lett. **97** (2006) 216803.
- [12] Y.W. Son, M.L. Cohen, and S.G. Louie, Nature (London) **444** (2006) 347.

- [13] L.D. Pan, L.Z. Zhang, B.Q. Song, S.X. Du, and H.J. Gao, *Appl. Phys. Lett.* **98** (2011) 173102.
- [14] J. Drogar, M.R. Roknabadi, M. Behdani, M. Modarresi, and A. Kari, *Superlattice Microst.* **75** (2014) 340.
- [15] M.S. Dresselhaus, G. Dresselhaus, and P.C. Eklund, *Science of Fullerenes and Carbon Nanotubes*, Academic, New York (1996).
- [16] R. Majid adn K. Ghafoori Tabrizi, *Physica B* **405** (2010) 2144.
- [17] R. Majidi, *Nano* **7** (2012) 12500231.
- [18] T. Ozaki, H. Kino, J. Yu, *et al.*, 2011, User's Manual of OpenMX Version 3.6. (<http://www.openmx-square.org>).
- [19] J.P. Perdew, K. Burke, and M. Ernzerhof, *Phys. Rev. Lett.* **77** (1997) 3865.
- [20] Y. Jing, G. Wu, L. Guo, Y. Sun, and J. Shen, *Comput. Mater. Sci.* **78** (2013) 22.
- [21] M. Long, L. Tang, D. Wang, Y. Li, and Z. Shuai, *ACS Nano* **5** (2011) 2593.
- [22] M. Büttiker, Y. Imry, R. Landauer, and S. Pinhas, *Phys. Rev. B* **31** (1985) 6207.
- [23] D. Ghosh, P. Parida, and S.K. Pati, *J. Phys. Chem. C* **116** (2012) 18487.
- [24] M. Modarresi, M.R. Roknabadi, and N. Shahtahmassebi, *Physica B* **415** (2013) 62.
- [25] M. Modarresi, M.R. Roknabadi, N. Shahtahmasbi, D. Vahedi, and H. Arabshahi, *Phys. E: Low-dimensional Syst. Nanostruct* **43** (2010) 402.
- [26] M. Ashhadi and S. Ketabi, *Physica E* **43** (2011) 851.